

DETERMINATION OF TENSION SOFTENING DIAGRAMS OF VARIOUS KINDS OF CONCRETE BY MEANS OF NUMERICAL ANALYSIS

Y. Uchida, N. Kurihara, K. Rokugo and W. Koyanagi,
Department of Civil Engineering, Gifu University, Gifu, Japan

Abstract

Poly-linear approximation method combined with FE-analysis using the fictitious crack model is introduced. The accuracy and validity of the method are examined by the numerical analysis. The poly-linear approximation method is applied to various kinds of concrete including porous concrete and fiber reinforced high strength concrete to determine the tension softening diagrams and also to certify the validity of the method.

1 Introduction

It was about twenty years ago that Hillerborg et al. (1976) proposed the Fictitious Crack Model (FCM). It is felt that the FCM is categorized into the old-fashioned model of concrete crack nowadays. However, the FCM has a sufficient ability to simulate the load-displacement response of the concrete members with the development of mode-I crack in spite of its simplicity. The most essential material property for the analysis using the FCM is the tension softening diagram, which is the relation between the decreasing transfer stress and the increasing crack opening in the fracture

process zone.

The standardized testing method to determine the fracture energy of the concrete by means of three point bending tests on notched beams has been proposed by RILEM (1983). On the other hand, the test method to determine the tension softening diagrams has not been standardized. Ideally, the simplest test method is to perform direct tension test. Unfortunately, it is not easy to control the crack propagation in the stable manner and symmetric way (van Mier (1986)). The following methods have been proposed: (a) direct tension test (Petersson (1981)), (b) data fitting technique (Roelfstra et al.(1986)) and (c) multi-cutting technique (Hu et al.(1989)). These methods and technique are still not easy to perform even in well-equipped laboratories. The J-integral based method proposed by Li et al. (1989) and the modified J-integral based method (Rokugo et al.(1989a), Uchida et al.(1991)) seem to be practical and easy methods, which require no special equipment or complicated program, although only rough softening diagrams could be estimated.

In this contribution, the poly-linear approximation method combined with FE-analysis using FCM is introduced and examined by the numerical simulation. The tension softening diagrams of various kinds of concrete are determined by the poly-linear approximation method and the validity of this method is discussed.

2 Poly-linear approximation method

2.1 Outline of poly-linear approximation method

Kitsutaka et al.(1993) proposed the poly-linear approximation method for determination of tension softening diagrams of concrete. This method is one of the data fitting method where the softening curve is determined to agree the analytical load-displacement curve with the experimental one. This method is different from Roelfstra's method.

In this method, the softening diagram is approximated by the poly-linear diagram and the coordinate of each knee point of softening diagram is determined step by step with the development of the fictitious crack in the analysis. Fig.1 shows the procedure for determination of $i + 1$ th knee point of the softening diagram where the knee points have been already determined until i th point. First, the linear softening $\bar{\sigma}(\omega)$ from i th knee point is assumed as shown in Fig.1(a). Next, the load, the displacement and the crack tip opening displacement (COD) are calculated when the fictitious crack tip has just reached to $i + 1$ th node in the analytical model (Fig.1(b)), and $\bar{\sigma}(\omega)$ is determined to agree the analytical load-displacement curve with the experimental one (Fig.1(c)). Then, the crack width at $i + 1$ th knee point ω_{i+1} is obtained as the analytical COD_{i+1} when $\bar{\sigma}(\omega)$ is determined (Fig.1(d)),

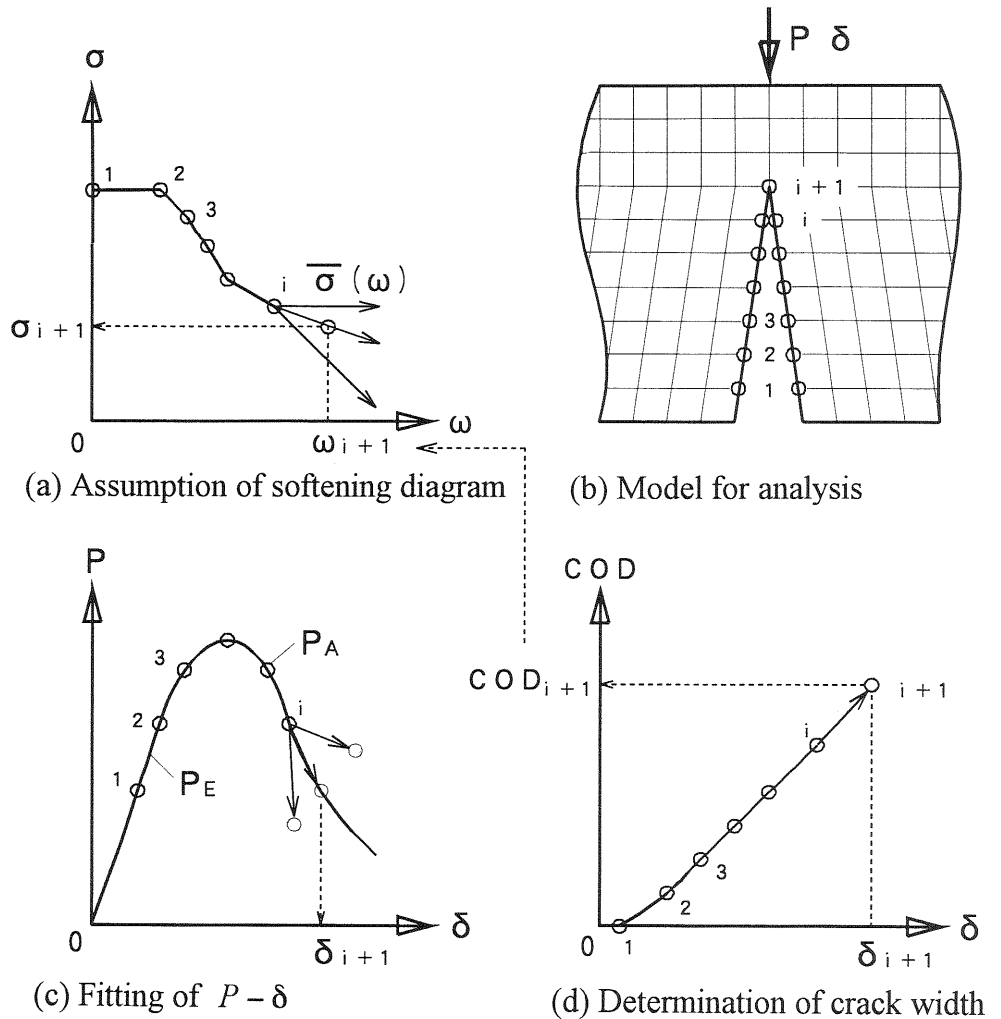


Fig. 1. Poly-linear approximation method

and finally, the stress at $i+1$ th knee point is obtained as $\bar{\sigma}(COD_{i+1})$ (Fig.1(a)).

The calculation program of the poly-linear approximation method is very simple, because it is only necessary to add the iteration routine to the crack extension analysis program using the FCM. Since the variable for the fitting is only the slope of $\bar{\sigma}(\omega)$, the iteration routine is also very simple. Furthermore, only stable load-displacement curves are needed to be measured in the experiment, and it does not matter what type of specimen is used. However, it is still problem to determine the tensile strength (start

point of softening diagram). The determination of the tensile strength is described in the following section.

2.2 Determination of tensile strength

Since the determination of tensile strength is also difficult in J-integral-based method, the split tensile strength is used as the tensile strength in the modified J-integral-based method. The tensile strength is determined from the maximum load in the original poly-linear approximation method by Kistutaka. It is certain that the maximum load of the specimen depends on the tensile strength of the concrete, but in the case of the other kind of concrete such as fiber reinforced concrete the maximum load depends on the bridging property of the fiber rather than the tensile strength of the matrix concrete.

For this reason, we assume the initial part of the softening diagram to be perfect plastic as shown in Fig.1(a). The tensile strength is determined to be the perfect plastic stress when the fictitious crack length becomes the longest within a given allowable difference between the experimental load-displacement relation and the analytical one. The allowable difference (*A.D.*) is given as

$$A.D. = \left| \frac{P_A(\delta_a) - P_E(\delta_a)}{P_E(\delta_a)} \right| \quad (1)$$

where δ_a is the displacement obtained through the analysis. $P_A(\delta_a)$ and $P_E(\delta_a)$ are the analytical and experimental loads corresponding to δ_a .

The Young's modulus used in this analysis is determined from the initial slope of load-displacement curve. The crack width of the end point of the perfect plasticity part is determined to be the crack opening displacement when the fictitious crack length becomes the longest. The knee points beyond the perfect plasticity part are determined by the method described in the previous section.

The method for the determination of tensile strength was examined through the numerical simulation. Fig.2 shows the finite element mesh of the left hand side of the beam specimen, which is $10 \times 10 \times 40$ cm and loaded at third point (loading span 30 cm). The 1/4 bilinear model (Rokugo et al.(1989b)) shown in Fig.3 was used for the FE-analysis of the load-load point displacement curve of the specimen and then the tensile strength and softening diagram were determined. Fig.4 shows the relation between the perfect plastic tensile stress (tensile strength) and the fictitious crack length. The tensile stress when the fictitious crack length becomes the longest depends on the allowable difference between the load-displacement curves,

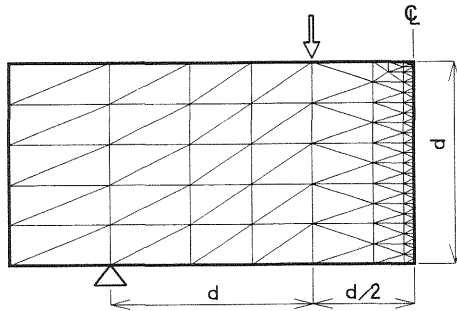


Fig. 2. Finite element mesh

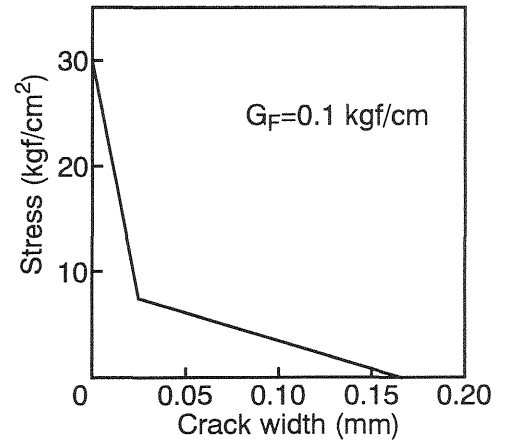


Fig. 3. Inputted softening diagram

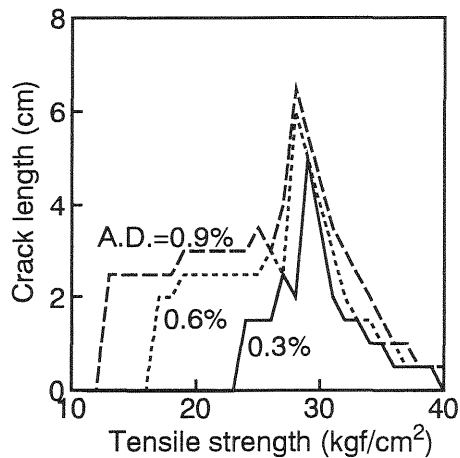


Fig. 4. Tensile strength and fictitious crack length

and a little smaller than the true tensile strength. This means that the adopted method gives only the rough estimation of the tensile strength.

Besides admitting the uncertainty of the tensile strength, the influence of the estimation error of the tensile strength on the determination of the whole softening diagram was examined. Fig.5 shows the estimated softening diagram with different initial perfect plasticity tensile stress (35, 29, 25 kgf/cm² (3.4, 2.8, 2.5 MPa)). The load-deflection curves were simulated

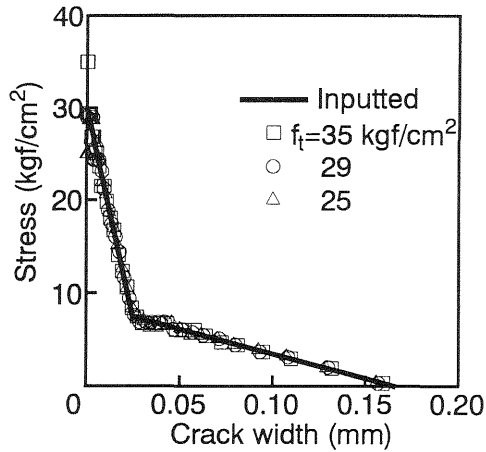


Fig. 5. Determined softening diagrams with different tensile strength

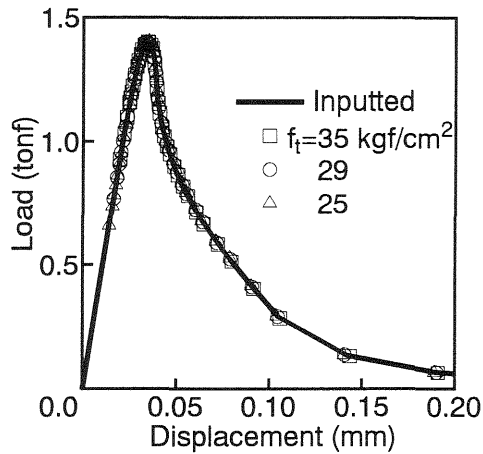


Fig. 6. Simulated $P - \delta$

through the FE-analysis using the determined softening diagrams and were shown in Fig.6. It is seen from Fig.5 that the estimated softening diagrams agree well with the true softening diagram, though the very initial part of the diagram depends on the tensile strength. All of the simulated load-deflection curves also agree well with the inputted load-deflection curve as shown in Fig.6. Consequently, it is not so important to determine the precise tensile strength for the determination of softening diagram by the poly-linear approximation method.

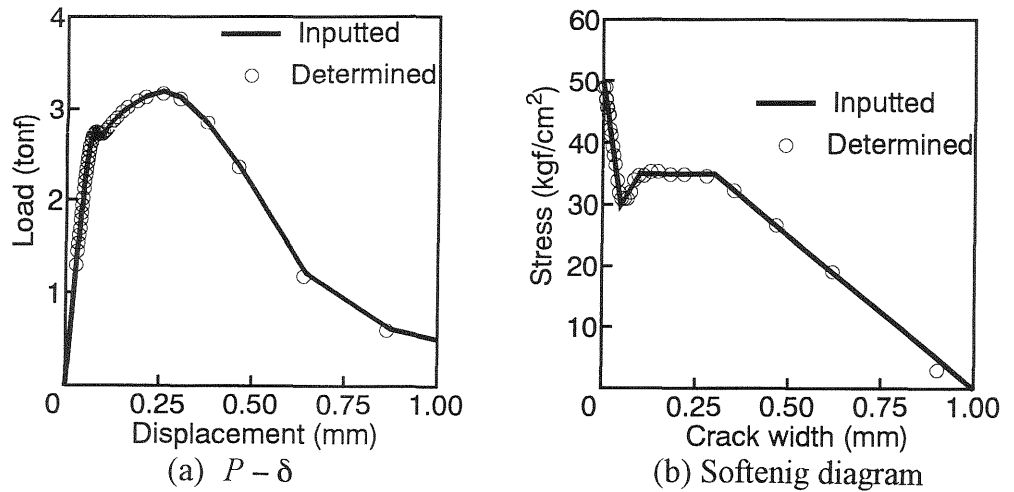


Fig. 7. Determined softening diagram of model FRC

Fig.7 shows the determined softening diagram assuming the fiber reinforced concrete. The poly-linear approximation method is effective for the another kind of concrete like the fiber reinforced concrete of which softening diagram has a quite different shape.

It is noted that we could not obtain the softening diagram if we had used the tensile strength which was extremely different from the true tensile strength. In this case the solution would diverge or oscillate. In our experience, the smoother softening diagram would be obtained if we used $(\omega_i + \omega_{i+1})/2$ instead of ω_i for the crack width of $i + 1$ th knee point described in section 2.1.

3 Tension softening diagram of various kinds of concrete

3.1 Plain concrete

The tension softening diagrams were determined through the modified J-integral based method and the poly-linear approximation method for the normal strength concrete, high strength concrete and light weight concrete. The loading tests were performed according to the RILEM testing method. The water cement ratio of the normal strength concrete, the high strength concrete and the light weight concrete were 0.53, 0.27 and 0.46, respectively. The maximum aggregate size was 15 mm. The weight of unit volume was 1.63 t/m³ for the light weight concrete. The compressive strength of the normal strength concrete, the high strength concrete and the light weight

concrete were 407, 848 and 344 kgf/cm² (39.9, 83.1 and 33.7 MPa), respectively. The size of beam specimen was 10×10×84 cm and the loading span was 80 cm.

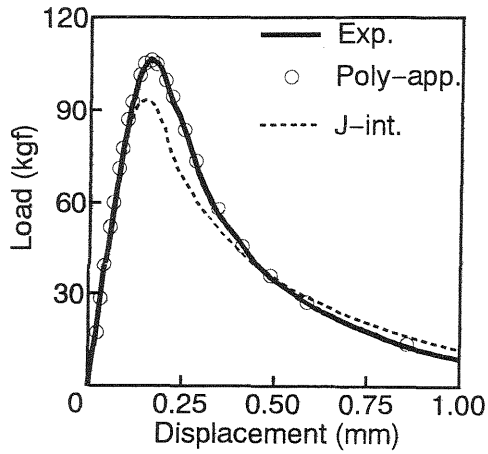
Fig.8 shows the load-deflection (loading point displacement) curves measured in experiment. Fig.9 shows the softening diagrams determined through the modified J-integral-based method and the poly-linear approximation method. The softening diagrams determined through the two methods are similar to each other. The load-deflection curves were simulated through the FE-analysis using the determined softening diagrams and are shown in Fig. 8. The simulated load-deflection curves using the determined softening diagrams through the poly-linear approximation method completely agree with the measured ones, whereas the load-deflection curves obtained from the modified J-integral-based method slightly differ from the measured ones.

The shapes of the tension softening diagrams of these concrete are similar to each other and might be modeled by bilinear function. Consequently, the data fitting technique assuming the bilinear function might be applied to these concrete.

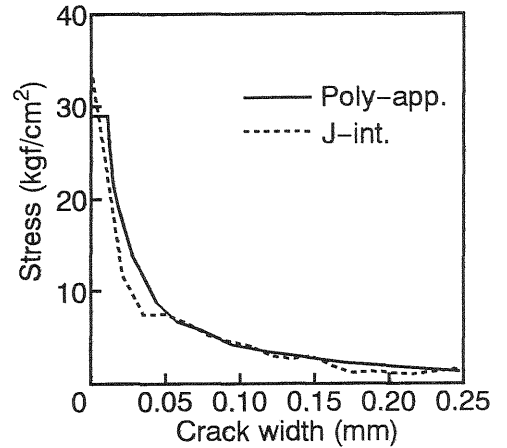
3.2 No-fines porous concrete

Since the crack opening displacement does not have to be measured when applying the poly-linear approximation method, the notch does not have to be made. The poly-linear approximation method was applied to the no-fines porous concrete beam specimen without a notch. The mix proportions were W:C:G = 47:289:1624 and the average compressive strength was 188 kgf/cm² (18.4 MPa). Three sizes of beam specimens were used. All the specimens had rectangular cross section with same width (10 cm). The heights of the cross sections were 10, 20 and 30 cm. These specimens are denoted as P10, P20 and P30, hereafter. The lengths of the specimen were four times the height. The loading span lengths in flexural test were three times the height. The third point loading test was carried out. Only the load-deflection (loading point displacement) curve was measured.

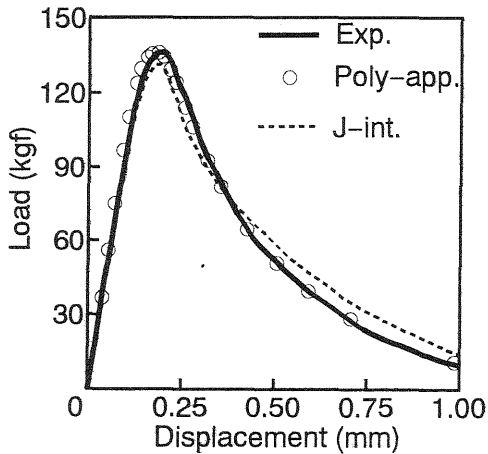
Fig.10 shows the load-deflection curves measured in experiment and Fig.11 shows the softening diagrams determined through the poly-linear approximation method. The clear difference of the softening diagram among the three sizes of specimens was not observed, whereas the longer tail of the softening curve was determined from the larger specimens. The load-deflection curves were simulated through the FE-analysis using the determined softening diagrams and are shown in Fig.10. The simulated load-deflection curves using the softening diagrams of the different specimens are also shown in Fig.10. The simulated load-deflection curves using the softening diagram of the same specimen completely agree with the measured ones. In case of P20 and P30, there is a little difference of the



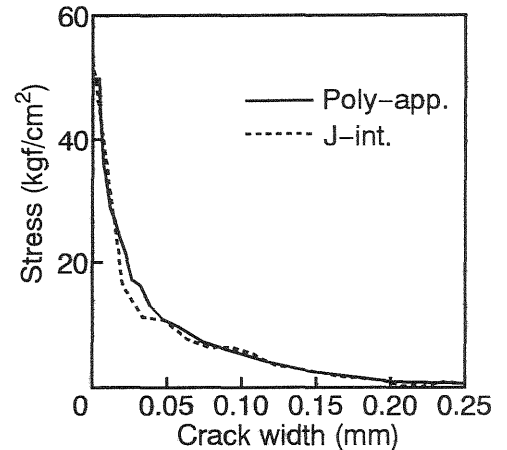
(a) Normal strength concrete



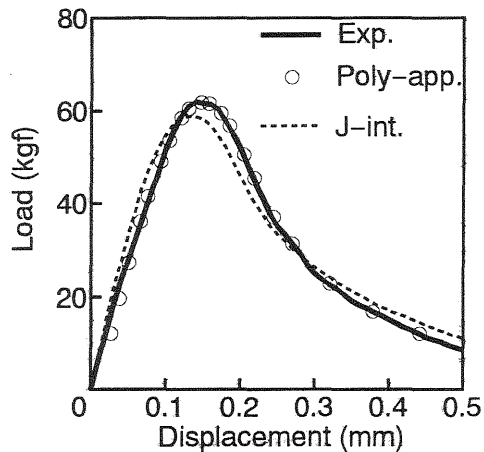
(a) Normal strength concrete



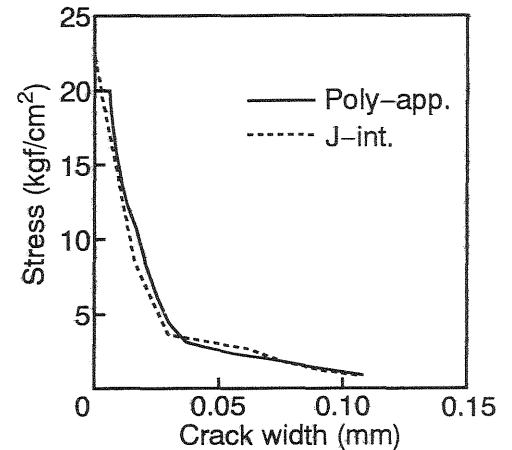
(b) High strength concrete



(b) High strength concrete



(c) Light weight concrete



(c) Light weight concrete

Fig. 8. $P - \delta$ of plain concrete

Fig. 9. Softening diagram of plain concrete

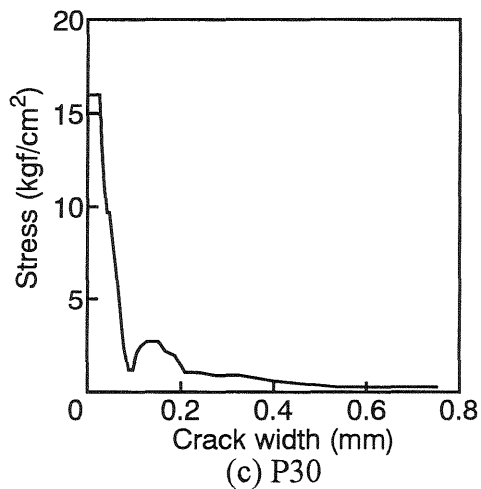
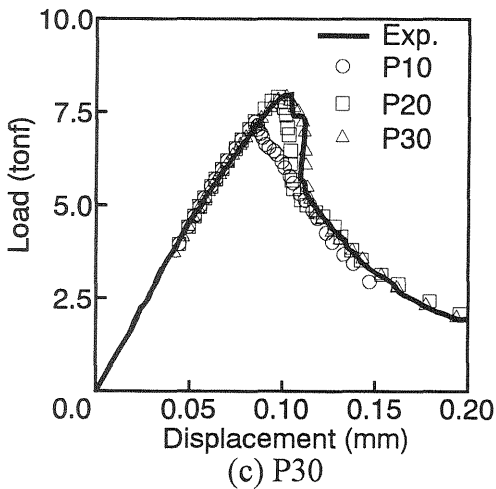
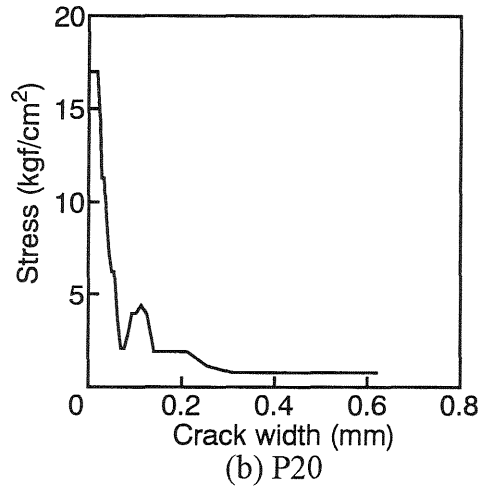
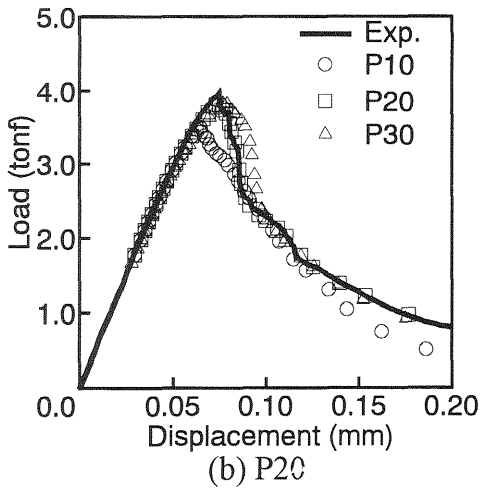
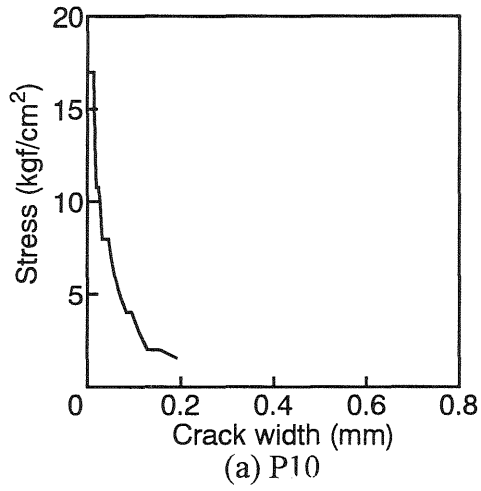
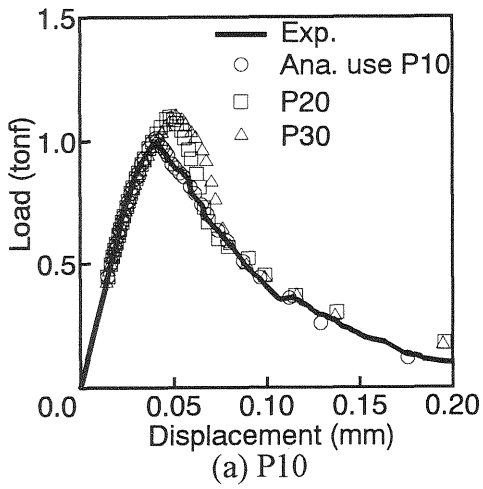


Fig. 10. $P - \delta$ of no-fines porous concrete

Fig. 11 Softening diagram of no-fines porous concrete

Table 1. Mix proportions and strengths of FRC

Concrete	Unit weight (kg/m ³)					Strength (kgf/cm ²)	
	W	C	S	G	F	comp.	flex.
AF	189	674	1348	-	28	859	134
VF	203	726	1276	-	28	827	109
SF	140	500	889	774	156	945	137

maximum load between the load-deflection curve using the softening diagram of P10 and the measured one.

3.3 Fiber reinforced high strength concrete

The tension softening diagrams were determined through the poly-linear approximation method for three kinds of fiber reinforced high strength concrete. Aramid fiber ($\phi 0.4 \times 30$ mm, strength: 3.0×10^4 kfg/cm² (2.9 GPa)), vinylon fiber ($\phi 0.38 \times 30$ mm, strength: 1.1×10^4 kfg/cm² (1.1 GPa)) and indented steel fiber ($\phi 0.6 \times 30$ mm, strength: 1.2×10^4 kfg/cm² (1.2 GPa)) were used. These fiber reinforced concrete are denoted as AF, VF and SF, hereafter. Volume content of the fiber was 2.0 %. The mix proportion and strength properties are shown in Table 1. The size of beam specimen without a notch was $10 \times 20 \times 70$ (width \times height \times length) cm and the loading span was 60 cm. The third point loading test was carried out, and the load-deflection (loading point displacement) curve was measured.

Fig.12 shows the load-deflection curves and Fig.13 shows the softening diagrams determined through the poly-linear approximation method. It is seen from these figures that the poly-linear approximation method is also effective for the fiber reinforced concrete. It is noted that the fracture energy of the aramid fiber reinforced concrete was about twice as large as that of the steel fiber concrete.

The shape of these fiber reinforced concrete might be modeled by trilinear function, that is, the initial softening part, the plastic part and the final softening part, as shown in Fig.14. These three parts would depend on the characteristics of the matrix concrete, bridging of fiber and pull-out or cut-off of the fiber, respectively.

4 Conclusions

Although it is difficult to determine the tensile strength precisely, the poly-linear approximation method is very effective for the determination of

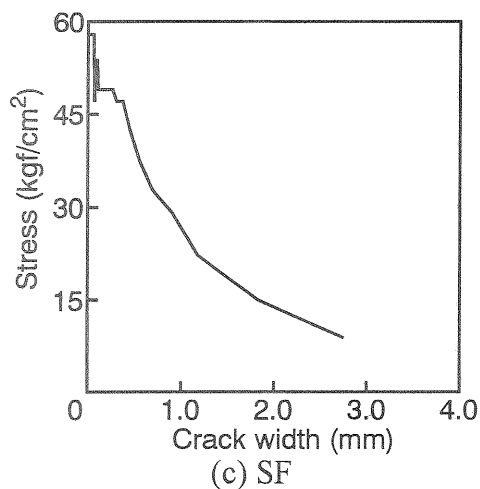
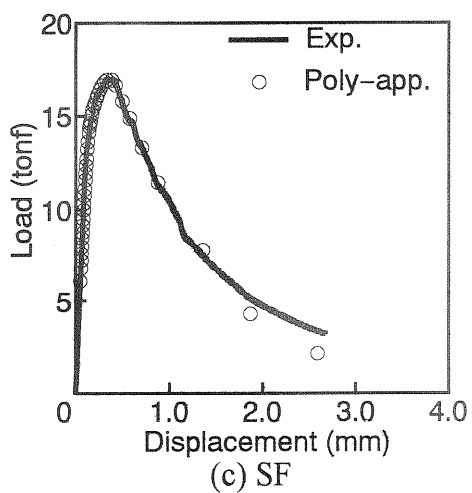
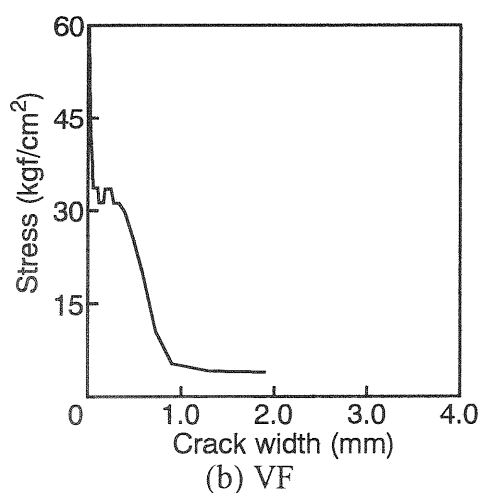
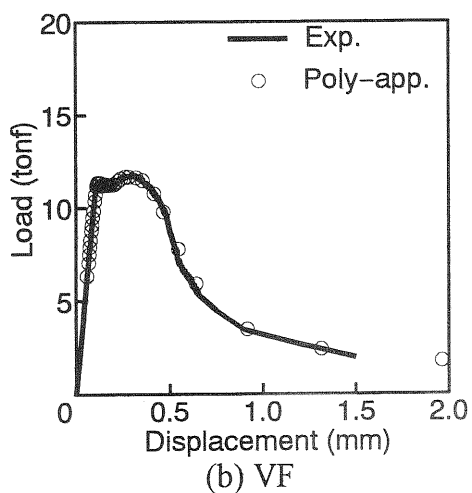
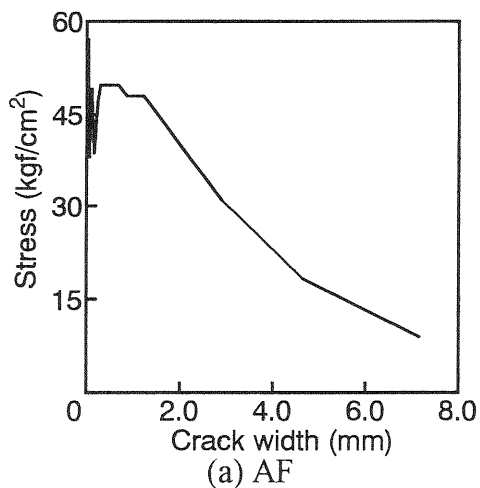
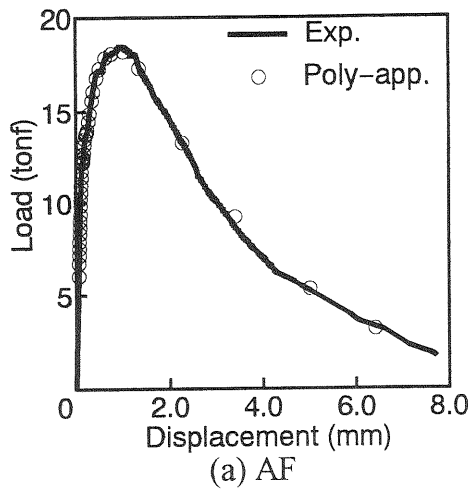


Fig. 12 $P - \delta$ of FRC

Fig. 13 Softening diagram of FRC

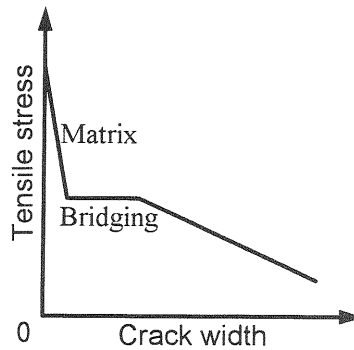


Fig. 14 Model of softening diagram of FRC

softening diagram of various kinds of concrete. The tensile strength is not so sensitive to the shape of the softening diagram determined through the poly-linear approximation method.

The numerical analysis is necessary in the poly-linear approximation method, but it is very easy to make the calculation program if we have the crack extension analysis program using the FCM. The combination of the experiment and numerical analysis would be one of trend of the evaluation method for the material properties.

5 Acknowledgment

The authors acknowledge the financial support for this study by the Kajima Foundation's Research Grant.

6 References

- Hillerborg, A., Modeer, M. and Petersson, P.E. (1976) Analysis of crack formation and crack growth in concrete by means of fracture mechanics and finite elements. **Cement and Concrete Research**, 6, 773-782.
- Hu, X.Z. and Wittmann, F.H. (1989) Fracture process zone and Kr-curve of hardened cement paste and mortar. in **Fracture of Concrete and Rock** (eds S.P. Shar, S.E. Swartz and B. Barr), Elsevier Applied Science, London, 307-316.
- Kitsutaka, Y., Kamimura, K. and Nakamura, S. (1993) Poly-linear approximation analysis of tension softening diagram for concrete. **J.**

- Struct. Constr. Engng**, Architectural Inst. of Japan, 453, 15-25.(in Japanese)
- Li, V.C. and Ward, R.J. (1989) A novel testing technique for post-peak tensile behavior of cementitious materials. in **Fracture Toughness and Fracture Energy** (eds H. Mishasi, H. Tkahashi and F.H. Wittmann), Balkema, Rotterdam, 183-195.
- van Mier, J.G.M. (1986) Fracture of concrete under complex stress. **Heron**, 31, 2-99.
- Petersson, P.E. (1981) Crack growth and development of fracture zone in plain concrete and similar materials. Report TVBM-1006, Div. of Building Mat., Lund Inst. of Technology.
- RILEM Draft Recommendation (1983) Determination of the fracture energy of mortar and concrete by means of three-point bend tests on notched beams. **Materials and Structures**, 18, 285-290.
- Roelfstra, P.E. and Wittmann, F.H. (1986) Numerical method to link strain softening with failure of concrete, in **Fracture Toughness and Fracture Energy of Concrete** (ed F.H. Wittmann), Elsevier Science Publishers, Amsterdam, 163-175.
- Rokugo, K., Iwasa, M., Seko, S. and Koyanagi, W. (1989a) Tension softening diagrams of steel fiber reinforced concrete, in **Fracture of Concrete and Rock** (eds S.P. Shar, S.E. Swartz and B. Barr), Elsevier Applied Science, London, 513-522.
- Rokugo, K., Iwasa, M., Suzuki, T. and Koyanagi, W. (1989b) Testing methods to determine tensile strain softening curves and fracture energy of concrete, in **Fracture Toughness and Fracture Energy** (eds H. Mishasi, H. Tkahashi and F.H. Wittmann), Balkema, Rotterdam, 153-163.
- Uchida, Y., Rokugo, K. and Koyanagi, W. (1991) Determination of tension softening Diagrams of concrete by means of bending tests. **Proc. Japan Soc. Civil Eng.**, 426, 203-212.(in Japanese) / **Concrete Library of JSCE**, 18, 171-184.